Reactivity at (nano)particle-water interfaces, redox processes, and arsenic transport in the environment.

Laurent Charlet, Guillaume Morin, Jérôme Rose, Yuheng Wang, Melanie Auffan, André Burnol, Alejandro Fernandez-Martinez

Réactivité aux interfaces (nano)particule-solution, processus redox et transport de l'arsenic dans l'environnement

Reactivity at (nano)particle-water interfaces, redox processes, and arsenic transport in the environment.

Laurent Charlet[1], Guillaume Morin[2], Jérôme Rose[3], Yuheng Wang[2], Mélanie Auffan[3] André Burnol[1,4], Alejandro Fernandez-Martinez[1,5]

[1] *ISTerre, Université Grenoble I and CNRS, PO Box 53, F38041, Grenoble* charlet38@gmail.com

[2] *IMPMC, UMR7590 CNRS-UPMC-UPD-IPGP, 140 r. Lourmel, 75015 Paris guillaume.morin@impmc.upmc.fr*

[3] *CEREGE, Université Aix-Marseille et CNRS, Europôle de l'Arbois, 13545 Aix rose@arbois.cerege.fr*

‘ *BRGM, avenue Claude Guillemin, BP 36009, 45060 Orléans Cedex 2, France a.burnol@brgm.fr*

[5] *Lawrence Berkeley National Laboratory, 1 Cyclotron Road, Mail Stop 90R1116, Berkeley, CA 94720, USA afernandez-martinez@lbl.gov*

Doit être soumis aux Comptes Rendus de l'Académie des Sciences

Abstract

Massive deleterious impacts to human health are resulting from the use of arsenic-bearing groundwaters in South-East Asia deltas and elsewhere in the world for drinking, cooking and/or irrigation. In Bangladesh alone, a fifth of all deaths are linked to arsenicosis. In the natural and engineered subsurface environment, the fate of arsenic is, to a large extent, controlled by redox potential, pH, as well as total iron, sulfur and carbonate content, via sorption and coprecipitation on a variety of natural and engineered (nano)particles. In the present article, we address: (1) new insights in the sorption mechanisms of As on Fe(II) and Fe(III) nanophases recognized to play an important role in the microbial cycling of As and Fe; (2) artifacts often encountered in field and laboratory studies of As speciation due to the extreme redox sensitivity of the Fe-As-O-H phases; and (3) as a conclusion, the implications for water treatment. Indeed the specific reactivity of nanoparticles accounts not only for the As bioavailability within soils and aquifers, but also opens new avenues in water treatment.

Résumé

L'utilisation dans les deltas du Sud-Est asiatique, et ailleurs dans le monde, d'eaux souterraines contaminées à l'arsenic pour boire, cuisiner et irriguer conduit à empoisonnement à grande échelle des populations locales. Pour le seul Bangladesh, un cinquième des décès serait lié à un empoisonnement à l'arsenic. Le devenir de l'arsenic dans les milieux souterrains naturels ou d'ingénierie est contrôlé par le pH, le potentiel d'oxydo-réduction et les teneurs en fer, soufre et carbonate de l'eau, par le biais de phénomènes d'adsorption et de coprécipitation à la surface de (nano)particules, tant naturelles que de synthèse. Dans cet article, nous discutons : (1) de nouveaux mécanismes d'adsorption de l'arsenic à la surface de ces nanoparticules, comme celles riches en Fe(II) et Fe(III) qui jouent un grand rôle dans le cycle biogéochimique du fer et de l'arsenic ; (2) des artefacts souvent rencontrés dans de telles études de laboratoire et de terrain, qui sont dues à l'extrême réactivité redox des systèmes Fe-As-O-H ; et (3) des implications quant au traitement de l'eau. En effet, la réactivité spécifique des nanoparticules non seulement rend compte de la biodisponibilité de l'arsenic dans les sols et les aquifères, mais elle ouvre aussi de nouvelles perspectives dans l'ingénierie du traitement de l'eau.

1. Background

a. Health Issues

Arsenic is a trace element which fate and bioavailability for plants and humans are strongly dependant on its speciation. Arsenic speciation and coordination are themselves strongly linked to redox conditions of the aqueous media, whether present in an aquifer or in a cell[1,2]. Ever since Neron who used arsenic to poison Claudius and Britannicus, arsenic has been well known for its acute toxicity to human beings, although it has also been used (and is still used) in China in the treatment of acute promyelocytic leukemia [3]. More recently, epidemiological studies in Chili and South East Asia have demonstrated its chronic toxicity in countries where daily chronic ingestion occurs via contaminated water and rice [4,5]. Consumption of drinking water containing 5 or 50 times the European Union (EU) and World Health Organization (WHO) Maximum Contaminant Level (MCL = 10 µg/L for As) induces a lung cancer risk equivalent to that of a passive or active smoker, respectively [4]. Other arsenicosis symptoms include hyperkeratosis, various forms of cancer (skin, bladder, and kidney), cardiovascular troubles, still birth and spontaneous abortion. Worldwide, 150 million people are at risk due to arsenic, among which 110 million are living in SE Asia deltas (Ganga-Bramapoutra, Mekong and Red River deltas), but other people at risk are living in desert areas and often depend on hydrothermal springs for their drinking water supply (e.g . inhabitants ofLos Angeles in the USA and Antofagasta in Chile), or are located downstream from mining activities [4, 6,7,8,9] In Bangladesh alone, 21.4% of all deaths and 23,5% of deaths linked to chronic disesases have been shown recently to be linked to the consumption of water with an arsenic concentration larger than the WHO MCL [10]

Arsenic bioavailability depends on its oxidation state, and each oxidation state (V, III or –III) corresponds to a specific coordination which will in turn dictate the fit of a given species within a given mineral structure or the ability of arsenic to cross a given biological barrier. The most oxidized form, As(V), corresponds to oxoanions with tetrahedral structure (arsenate ions). In suboxic to mild reductive environments, the dominant form is As(III)which corresponds to aqueous arsenite species characterized by a pyramid geometry (trigonal coordination). In extremely reductive biological environments (in human liver or red cells) arsenic may be biotransformed to arsenide (As(-III)) species [3, 11, 12]; For instance, *E. coli* cells have been recently demonstrated to be able to produce the highly toxic gaseous form arsine, AsH_3(g), as well as other methylated As(-III) species [13]. Eventually, a variety of methylated As(III) and As(V) species [14], as well as (seleno)glutathione-As(III) complexes

are commonly produced in living organisms, these latter molecules playing a key role in As detoxification processes [2,11,12,15,16]. Similar reduction mechanisms occur in anoxic surface environments (peat bogs, paddy fields, stratified lakes)

b. Mineralogical vs. biological control of As scavenging and release

Within the complexity of deltaic hydrology and geochemistry [17,18], the predominant nano mineral phase changes over distances of 100 m (A. Foster, Pers. Comm.) Wherever overlying sandy soils allow a direct vertical recharge of the groundwater, down to 60 meters in less than 60 years [19], Fe(III) oxyhydroxide and oxyhydrosulfate nanoparticles may induce the trapping of arsenic in these oxic/suboxic grey sediments., [17]. On the other hand, wherever an overlying impermeable soil leads to anoxia in the aquifer located below mobilization of arsenic in the aquifer occurs. The Fe(II/III)-rich nanophases formed in these conditions (e.g.mackinawite and magnetite) are comparatively poor arsenic sorbents. The concentration of arsenic in groundwater is therefore strongly related to the mineralogy, pH, and Eh as well as to bacterial activity [20, 21, 22] (Figure 1).

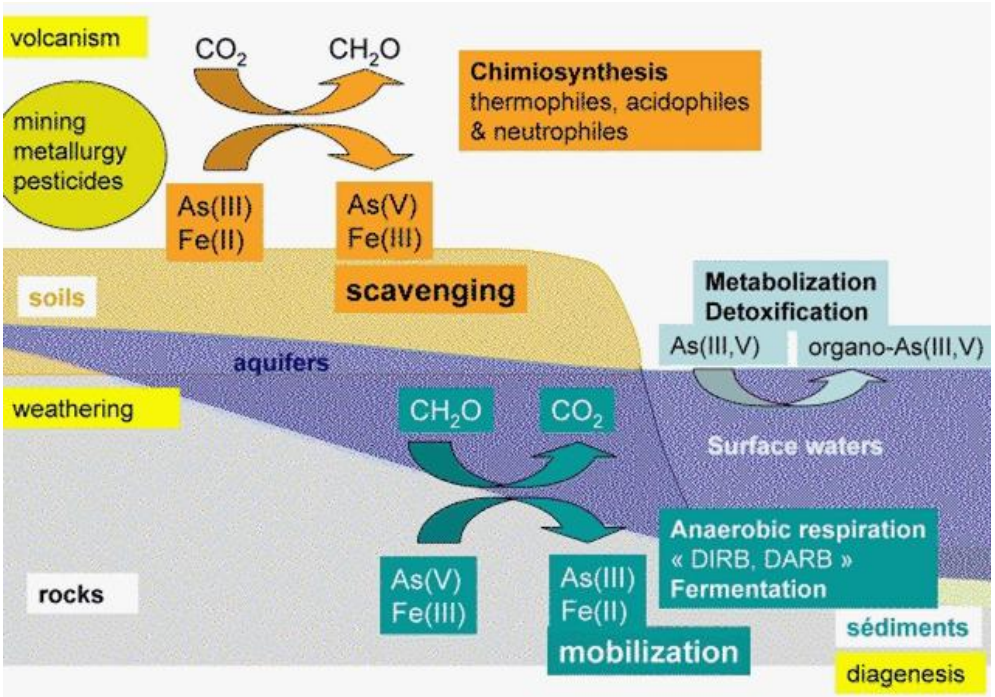

Figure 1. Simplified sketch of arsenic cycling in the environement, showing the influence of microbial metabolisms on iron and arsenic oxidation states. Oxidation reactions are generally associated to scavenging of As(V) by insoluble Fe(III)-oxyhydroxides and

oxyhydroxysulfates, while the reductive dissolution of these latter phases, for instance by Dissimilatory Iron and/or Arsenic Reducing bacteria (DIRB, DARB) is generally associated to the release of the highly toxic As(III) form in the aquifers.

Similarly, field and laboratory investigations performed over the last twenty years of oxic soils and mining environments have shown arsenic to be scavenged in oxic conditions by Fe(III) oxyhydroxides (e.g. [23,24] and references theirein), while in anoxic conditions Fe(II) and As(III) tend on the long term to be released in the aqueous phase [25], even though the process can be delayed by arsenic sorption on Fe(II)-rich phases (green-rusts, magnetite, pyrite, troilite and mackinawite) [26,27,28,29]. Even if a full understanding of the mobilization of arsenic in groundwater is far to be achieved, the large body of recent literature delineates thesemechanisms as mechanisms controlling the fate of arseic in soils and aquifers..

Cconsumption of dissolved oxygen and nitrate preceeds the reduction and dissolution of Mn and Fe oxides (see e.g. [29]) and in West Bengal groundwater, the consumption of nitrates preceeds the reduction of sulfate and Fe oxides [29]. However, on a short term basis, Fe and As releases may not occur simultaneously, ([20,21,30]). Van Geen et al. [21] have shown that truly anoxic conditions may indeed not be required for the release of As from reducing grey sediment in Bangladesh. In two months long experiments run with unamended gray sediments from Bangladesh, they observed a gradual release of the equivalent of 0.5 to1.0 µg/g As to the dissolved phase even in the presence of some dissolved oxygen (~1 mg/L).. They showed consequently that a release of significant amounts of arsenic may occur without the need for extensive Fe dissolution suggesting that the release of As and Fe is decoupled. Burnol et al. [20] demonstrated by microcosm studies and dynamic equilibrium modeling that this discrepancy is controlled by chemistry rather than by microbiology. When arsenic-rich, 1-5 nm wide ferrihydrite particles [31] are dissolved by the iron-reducing bacteria, aqueous Fe^{2+} concentration increased and Eh first decreases while no arsenic appears in solution (Figure 2). This process is interpreted as an immediate readsorption of the As(V) released by the As rich ferrihydrite coprecipitate reductive dissolution, on other ferrihydrite particles. When Eh reaches the As(V)/As(III) boudary limit, arsenic is reduced to As(III). Since this form is in these experimental conditions more weakly adsorbed than As(V) in presence of carbonates, As appears in solution, in an apparent “decoupled” manner , but in fact thermodynamically perfectly coupled to the release of Fe(II) in solution (Figure 2). In an alternative scenario, an Fe-bearing phase may dissolve and in the process release As, while another As-poor, Fe-

bearing phase (e.g. a phosphate like vivianite) could precipitate kinetically [20]. This alternative scenario could account for the lack of evidence for As being released into solution during the early Fe release (G. Brown, pers. Comm.). Whatever the final interpretation, microorganisms are clearly playing a central role in As release, as demonstrated by experiments run with the same sediment treated with a cocktail of penicillin G, chloramphenical and streptomycin antibiotics (Guillard reagent), in whicho arsenic release was observed in these mesocosms [21].

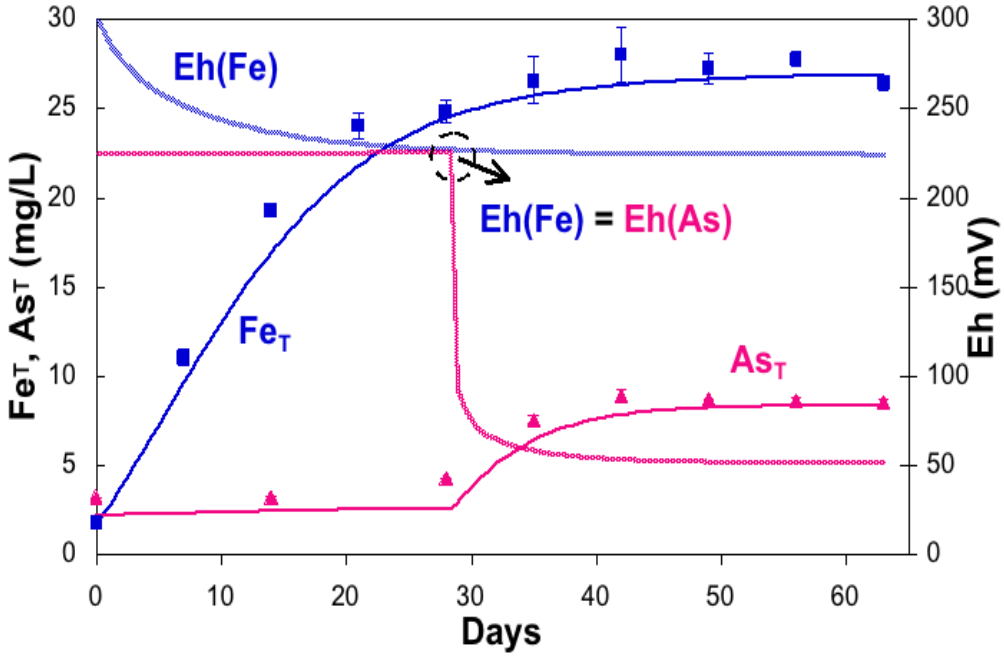

Figure 2. Decoupled release of Fe(II) and As(III) in a microcosm experiment and the dynamic equilibrium model (see text**)** (after [20])

Microbially driven reductive dissolution of ferric iron hydroxide (goethite, ferrihydrite or lepidocrocite) in the presence of organic matter and CO_2 can be written simplistically as:

$$CH_2O + 7CO_2 + 4\ FeOOH = 4\ Fe^{2+} + 8\ HCO_3^- + 3H_20$$

The age of DIC (HCO_3^- ions) and DOC ("CH_2O') may be differentiated by a combination of $^{13}C/^{12}C$ and $^{14}C/^{12}C$ measurements. In Cambodia and in Indian delta groundwaters the water DIC was found to be much younger than the DOC [19], therefore not being formed only by the above chemical reaction. DOC is therefore also not primary derived from modern surface organic matter. Since it is negatively charged, DOC may not only act as electron donor, but also as direct competitor with arsenic anionic species for sorption on the iron oxyhydroxide particles.

The bicarbonate ions produced in the above reaction may further lead to the formation of siderite ($FeCO_3$). Cambodian and Indian arsenic affected groundwaters are often oversaturated with respect to siderite precipitation by an order of magnitude [32,33]. In presence of excess bisulfide ions, mackinawite (FeS) and other FeS_x (with $1<x<2$) may form. Flow-through reactor studies performed on soil synthetic aggregates (made of ferrihydrite, quartz sand, *Shewanella sp*. iron-reducing bacteria and agarose) lead to contrasting results depending on whether As is present or not in water. When the system was amended with a 0.3 mM lactate solution without arsenic, the development of an anoxic environment in the heart of the aggregate was observed after three months of bacterial activity [34,35] with micron-sized siderite particles in the heart of the aggregate. However, when arsenic was added to the lactate solution, no siderite was formed [36]. Some magnetite was also produced at the surface of the aggregate but not in the core region. These dynamic experiments demonstrate differential secondary product formation: siderite, together with α/γFeOOH forms in the core region of the aggregate where more reducing conditions prevail, and magnetite forms at the surface of the aggregate. The nanosize of most of these products also explains why XRD rarely provides evidence for the formation of magnetite and siderite in SE Asia deltaic aquifers, while diffuse reflectance measurements points to the presence of Fe(II)-rich solid phases [21].

On the other hand, in soils where oxic conditions prevail, i*n situ* speciation of As investigated by combining X-ray Absorption Spectroscopy (XAFS) with selective chemical extractions demonstrated As to be mostly present as surface complexes on iron oxides in soils [e.g., [23] and references therein]. Although, the relative importance of phyllosilicates as arsenic sorbents is generally difficult to evaluate in soils, the lower affinity of As(III) for Al-bearing phyllosilicate minerals compared to iron oxyhydroxides [37] could be responsible for the increased As(III) mobility in iron-depleted anaerobic media.

In acid mine drainage [23,38] and geothermal springs [39] XAFS studies have revealed a similar coupling between arsenic and iron chemistry in these extreme environments. In both contexts, microbial oxidation of Fe(II) and As(III) leads to the formation of amorphous As(V)-Fe(III) hydroxysulfate compounds with similar local structure [40]. Thehe solubility of these compounds directly decreases with increasing Fe/As ratio (Figure 3). As(V)-Fe(III) hydroxysulfate minerals are frequently associated with biological substances, and could be considered as potential markers of microbial activity in extreme acidic environments. The role of microbial oxidation is especially important for the kinetics of Fe(II) oxidation, which is low

in acidic environment and may directly influence the nature of the biogenic minerals formed [41]. The ability of arsenic resistant anaerobic iron oxidizing microorganisms to immobilize As by sorption on biogenic Fe(III) oxyhydroxides in anoxic conditions, have been further recently demonstrated in laboratory experiments [42]

2. Sorption: Kd and species-specific mechanisms of As sorption

Sorption of As onto a mineral particles can be characterized macroscopically by the observed Kd (g/L) value, defined as the ratio measured at a given pH and ionic strength between the total aqueous As concentration (mol/L) and the solid As concentration (mol/g). Table 1 reports Kd values measured at pH 7 or pH 7.5 (i.e. in the pH range of most SE Asia As-contaminated groundwaters) at various solid/solution ratios. Clearly, the As(V) and As(III) Kd values differ. For example, Kd values are sometimes higher for As(III) (for sorption on ferrihydrite, goethite) than for As(V), and sometimes lower (for sorption on mackinawite, siderite, magnetite or biotite). Magnetite and mackinawite have similar Kd values. Those Kd values for Fe(II) rich minerals are particularly important since pure Fe(III) oxyhydroxides (e.g. ferrihydrite and goethite) are seldom observed in anoxic deltaic aquifers throughout SE Asia, but instead diffuse reflectance spectra consistently show the presence of fine-grained Fe(II)-bearing minerals in these porous media [17]

Recent studies using XAFS spectroscopy, neutron diffraction, HRTEM, and DFT molecular modeling, have revealed, as will be discussed in the following sections, the formation of a large variety of arsenic surface complexes upon sorption onto ferric oxyhydroxides [44,48], nanomaghemite [49;50], nano-magnetite [51,52,53], iron hydroxycarbonates [54], mackinawite [44], calcite [55] and gypsum [56]. Arsenite forms a specific tridentate, triple corner-sharing surface complex both with magnetite [52,53] and maghemite [49], which explains, in part, the high adsorption affinity of arsenite for these substrates. In addition, a "nano" effect is observed for magnetite which may sorb 0.021, 0.388 and 1.532 mmol g^{-1} of arsenite, i.e. 5-6 µmol m^{-2} to 18 µmol m^{-2}, for particle sizes decreasing from 200 nm to 20 and 12 nm [51, 49, 53]. Although the origin of this increased reactivity is still a matter of debate, it will be shown to be attributed either to an increased surface tension [54,55] or to surface precipitation of arsenite [53]. Polymeric arsenite surface complexes may also form on green-rusts and may play an important role in delaying the release of arsenic in suboxic soils [54, 56]. Even though electron transfer between structural Fe(II) and arsenate species is not observed on green-rusts [52], arsenate may be reduced by Fe^{2+} sorbed on micas

and clays [57]. In the case of carbonate and sulfate minerals, isomorphic substitution of the constitutive anion by the appropriate arsenic oxoanion may enhance sorption as well [58,59].

a. Ferrihydrite, goethite, and As(V) adsorption: Alternative spectroscopy and modes of sorption

Thanks to more than two decades of laboratory studies, sorption of arsenate at the surfaces of common ferric oxyhydroxide minerals, especially goethite and ferrihydrite, has been demonstrated to be one of the most efficient trapping processes for dissolved arsenate [60,61], and many water purification processes utilize this process (after a first step of chemical or biotic oxidation of arsenite to arsenate). Several studies addressing arsenic speciation in contaminated environments have also shown that this process is active in the field (e.g., [23,62] and references therein). Comparison of natural As-bearing soils with polluted ones have shown that arsenate binding to poorly ordered ferric oxyhydroxides, such as ferrihydrite, retards As transfers toward surface- and ground-waters in the oxic zone whenever crystalline arsenate minerals are not less stable and therefore do not retain arsenate ions in long-term weathering processes [63,64] (Figure 3). At the beginning of this millenium, much less data was available on the behavior of the toxic As(III) form, and extensive research has been conducted on the interactions of this species with the ferric oxyhydroxide surfaces (e.g. [61]). A XAS-based study conducted by Ona-Nguema et al. [65] compared the modes of As(III) sorption onto 2-line ferrihydrite, hematite, goethite, and lepidocrocite. Sorption experiments and spectroscopic data acquisition were performed under anoxic conditions in order to minimize As(III) oxidation due to reactive oxygen species. These EXAFS data indicate that As(III) surface complexes on hematite and ferrihydrite are similar, but they differ significantly from those on goethite and lepidocrocite. The main difference is the absence of bidentate edge-sharing complexes (^2E) at the surface of the two latter minerals. This ^2E complex, which is characterized by a short As-Fe distance of 2.9 Å, appears to be specific to the As(III)O_3 pyramid geometry, since it has been demonstrated by several recent studies that this complex actually doesn't form in the case of the tetrahedral As(V) species (e.g., [50,56,66,67,68]). It was indeed shown that, in the case of As(V), As-O-O and As-O-O-O multiple scattering path contributions to the EXAFS had been long misinterpreted as being due to a ^2E complex **(**e.g. [66, 67]**)**. These findings are consistent with the known structures of ferric arsenate and arsenite minerals in which the ^2E linkage is only observed for arsenite (e.g., [40]).

Despite these significant advances in understanding the mode of arsenic binding at the surface of ferric oxyhydroxides, several questions are still open and may have important implications for properly modeling As sorption reactions. The main recent important finding provides clear evidence for both outer-sphere and inner-sphere As(V) complexes at the hematite/aqueous solution interface demonstrated using Resonant Anomalous X-ray Reflectivity (RAXR) by Catalano et al. [69]. These RAXR results show that about 35 percent of the sorbed arsenic occurred in the outer-sphere form in the hematite samples studied. The exact nature of theses outer-sphere complexes is still poorly constrained, but several lines of evidence suggest that they could correspond to hydrogen-bonded species, which would explain the fact that they are not displaced with increasing ionic strength. Such outer-sphere complexes are extremely difficult to detect using EXAFS spectroscopy in the presence of inner-sphere As(V) complexes because their presence is manifested by average As(V)-OH_2 distances that do not differ significantly from the average As(V)-O distances in inner-sphere As(V) complexes to allow their unambiguous distinction the two. In addition, although the As(V)-Fe(III) distances of outer-sphere As(V) complexes at hematite/water interfaces are significantly longer than those of inner-sphere As(V) complexes, the integrated intensity of this feature in the radial distribution function should be significantly weaker than that of the As(V)-Fe(III) pair correlation due to inner-sphere complexes. As a result, the presence of outer-sphere As(V) complexes at Fe(III)-oxide/aqueous solution interfaces could have been underestimated in past laboratory and field studies or missed altogether. Grazing-incidence EXAFS (GI-EXAFS) spectroscopy is also able to detect outer-sphere complexes, as demonstrated by a study [70] on Pb(II) sorption onto α-Al_2O_3 (0001) single crystal surface in contact with water. A major limitation of both RAXR and GI-EXAFS studies, however, is that they can only be conducted on species sorbed on single crystal substrates, which are not representative of the fine-grained, high surface area minerals and mineraloids that are typical of most natural environments. More experimental and theoretical work is needed to better understand the nature and importance of these outer-sphere complexes for both As(V) and As(III).

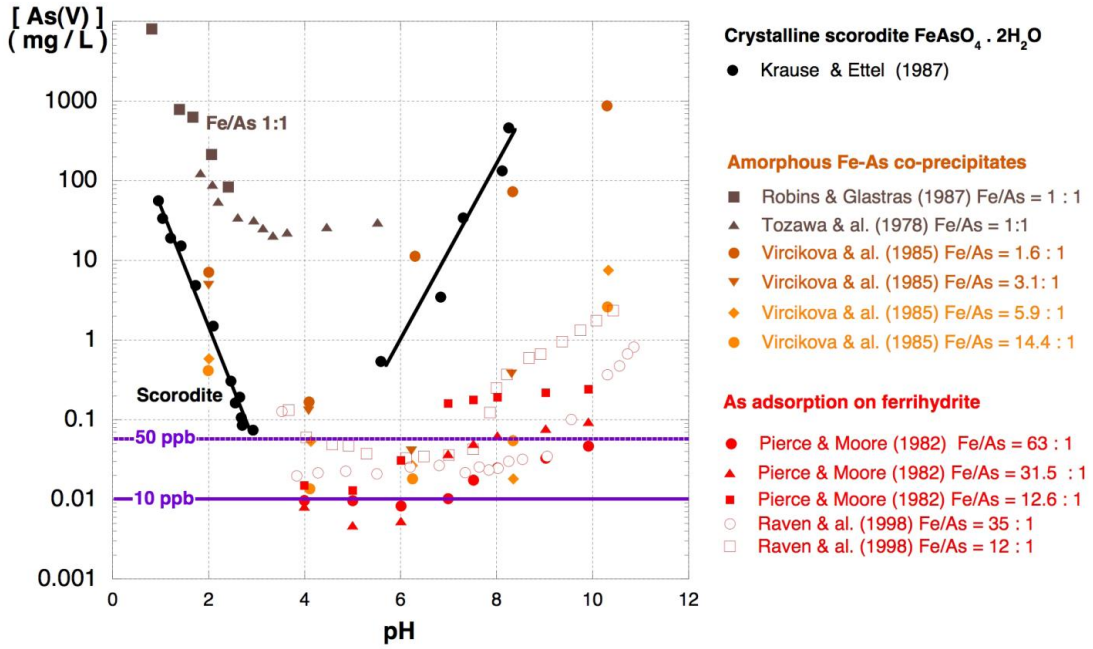

Figure 3. Solubity of crystalline and amorphous hydrated ferric arsenate mineral phases compared to that of As(V) sorbed on ferrihydrite. At low Fe/As ratio the crystalline phase is less soluble than the amorphous or nanocrystalline ones. The As solubility significantly decreases with increasing the Fe/As ratio, and the lowest solubility values are obtained for As(V) species sorbed on ferrihydrite surface, which yield dissolved As concentration below the WHO Recommended drinking Limit (10 ppb).

b. Magnetite and maghemite: nanoparticle size and site specific effects on As sorption

As discussed above, iron oxides and iron oxy-hydroxides are strong sorbents for many metals and metalloids such as arsenic. At given physico-chemical conditions (pH, ionic strength metal ion concentration, reactive surface area of sorbents), the sorbed quantity of the metal or metalloid will depend on the nature of the iron mineral. Although the thermodynamic constants of sorption will vary as a function of iron oxide or oxy-hydroxide composition (Table 1), the adsorbed quantity can also be size dependent for a given mineral. Indeed, for the specific case of magnetite, a potentially important sorbent for arsenic in reducing environments as well as in putative remediation processes, especially for the reduced and highly toxic As(III) form, the quantity of arsenic per gram strongly increases from 0.02 mmol/g of arsenic for 300nm particles up to 0.38 mmol/g for 20 nm magnetite and 1.8 mmol/g for even smaller 11 nm wide magnetite particles [77]. Such a significant increase in amount of arsenic adsorbed on nanometric particles may be related to strong modifications of

other properties like surface structure and surface reactivityas size decreases [49,78]. All of these potential modifications of particle properties as size reaches the nano domain have been generalized as 'nano-effects' and are at the origin of the exiting emerging scientific field of nanotechnology.

Concerning the arsenic adsorption example, identification of a nano-effect cannot result from a comparison of the amount of As adsorbed per mass of particles. Indeed such strong increases are not surprising since the specific surface area (SSA) of particles is inversely proportional to the size of particles, assuming that nanoparticle aggregation is minimal. For instance for the latter example, the SSA increases from 3.7 to 60 to 98.8 m^2/g for 300, 20, and 11 nm magnetite particle diameters, respectively. Therefore, to further investigate the possibility of a 'true' nano-effect, one must compare the adsorbed quantity not per mass but per surface area [54]. When sorption is expressed per unit of surface area, magnetite particles of 300 and 20 nm diameter adsorbed similar amounts of As (i.e., 3.5 As/nm^2) suggesting similar adsorption mechanisms. Therefore, the difference in As uptake between the 20 and 300 nm magnetite particles is only related to the SSA. In stark contrast, the adsorption capacity increases particles get smaller than 20 nm, and 11 nm-diameter magnetite adsorbs 3 times more As per square nanometer (10.9 As/nm^2) than does 20 and 300 nm-diameter magnetite.

We have recently observed a similar effect for arsenite adsorption at the surface of maghemite [49]. In that study, 6 nm-diameter maghemite particles were shown to adsorbed up to 8.1±0.8 As per nm^2. Such a 'nano' effect raises questions about the mechanisms of metal ion adsorption on nano-sized mineral particles, particularly the possibility that the surface atomic structure of nanoparticles in the smallest size range is potentially different than that of larger sized particles of the same material, which could lead to significant differences in reactivity. A combination of sorption experiments and characterization studies of the evolution in nanoparticle structure and As local atomic environment has lead to the identification of two main phenomena that may help explain the origin of these observed nano-effects. The first factor is related to a size-dependent structural modification of the surface of particles. Brice-Profeta et al. [79] have shown that the occupation rate of the maghemite tetrahedral site by Fe ($[Fe_{Td}]$) decreases as particle size decreases. This study has also demonstrated the existence of a preferential iron octahedral layer at the nano-maghemite surface, i.e. a deficit of Fe_{Td} at the surface of very small maghemite nanoparticles. X-ray diffraction revealed that before As(III) adsorption, 10% of Fe_{Td} sites are vacant. The adsorption of As(III) led to an increase in the occupancy of the surface Fe_{Td} sites, as revealed

by X-ray diffraction, suggesting possible As adsorption at this very specific maghemite crystallographic surface sites. EXAFS at the As K edge further indicated that As was chemically sorbed but with a surprising high Fe coordination number (3.1 ±0.6). A careful examination of the coordination of the [Fe_{Td}] site on the {111}, {011}, and {100} surface planes strongly suggested that As filled the [Fe_{Td}] surface sites through the formation of tridentate, hexanuclear, corner-sharing (^3C) surface complexes. Morin et al [53] found the same As(III) complex at the surface of magnetite in sorption as well as coprecipitation experiments [52] (Figure 5). At higher surface coverage, arsenite adsorbs on Fe octahedral [Fe_{Oh}] surface sites through monodentate trinulear complexes supposedly in a lattice position.

Even if adsorption of As(III) at the highly reactive vacant surface [Fe_{Td}] sites on magnetite and maghemite can explain the uptake of ~ 2 As/nm^2, it can not explain the maximum amount observed for As adsorption (8 As/nm^2). Other factors need to be taken into account to help understand this unusually high level of As(III) uptake. Indeed nanoparticles are thermodynamically unstable compared with their microscopic counterparts. Adsorption of ions at the surface of particles decreases the energy ($\underline{\Delta}G$) of a system by $\Delta G = 3V_m\Delta\gamma/r$, where V_m is the molar volume, $\Delta\gamma$ is the difference in interfacial energy before and after adsorption, and r is the radius of the particles. Therefore the adsorption of a dense arsenite layer decrease - via radius increase - the energy of the system more than when adsorption occurred on larger particles of 20 or 300 nm. Whereas in macroscopic systems adsorption is mainly governed by chemical affinity and electrostatic bond strengths, for nanoparticles the decrease of free energy must be taken into account. This driving force is known to be predominant in the case of crystal growth. In our past studies, the adsorption of As^{III} in the vacant [Fe_{Td}] lattice positions at the nano-maghemite surface can be compared to a crystal growth mechanism in which As^{III} mimics the [Fe_{Td}] atoms. This may explain the high density of As adsorbed at the surface of nano-maghemite.

.

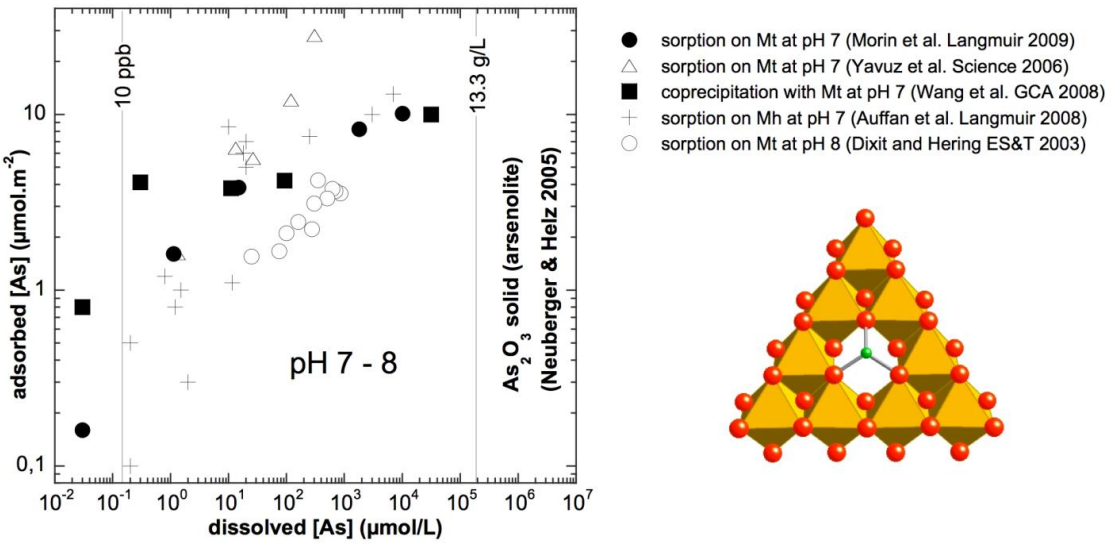

Figure 4. Isotherm data for As(III) sorption on magnetite [43], nanomagnetite [83,84] and nanomaghemite [49], compared with data for As(III) coprecipitated with magnetite [52] . The tridentate As(III) surface complex on the (111) facet of magnetite/maghemite model responsible for the high affinity of As(III) for these mineral surfaces and, derived from EXAFS spectroscopy by [49,52,84]. is shown on the bottom right. Arsenic and oxygen atoms, and iron octahedra are displayed in green, red and orange color.

c. Magnetite: surface precipitation of As

The large amount of As adsorbed at the surface of iron oxide nanoparticles may also have another origin. Morin et al. [53] have shown that in the case of 11 nm nano-magnetite particles as well as for the 34 nm particles, the high surface coverage is due to the formation of an amorphous As(III)-rich surface precipitate. This explains why nanocrystalline magnetite (< 20 nm) is found to exhibit higher efficiency for arsenite sorption than larger magnetite particles, sorbing as much as ~10 µmol/m^2 of arsenite [83]. Recent X-ray absorption spectroscopy studies[53,52] have demonstrated that, when sorbed on, or coprecipitated with, magnetite at neutral pH, As(III) forms dominantly inner-sphere, tridentate, hexanuclear, corner-sharing surface complexes (^3C) in which AsO_3 pyramids occupy vacant tetrahedral sites on octahedrally terminated {111} surfaces of magnetite. A similar geometry was observed by Kirsch et al. [85] for Sb(III) sorption complexes on magnetite, as well as by Auffan et al. [49] for As(III) sorption complexes on nanomaghemite (see previous section). Upon As(III) sorption on magnetite below surface coverages of 0.2 µmol/m^2, the observed

dissolved As(III) concentration is below the Maximum Concentration Level recommended by the World Health Organization (10 µg/L) [84].

The sorption mechanism may then be related to a modification of the nanoparticle surface involving dissolution of a fraction of the surface iron atoms and coprecipitation of an amorphous solid with arsenite. Such a mechanism has already been observed for Co(II) sorption on γ-Al_2O_3 [80], for Ni(II) sorption on Al_2O_3 [81], and in the case of selenite adsorption on magnetite [82]. Such a mechanism may be less important in the case of As(III) adsorbed on nano-maghemite particles because Fe(III) solubility is several orders of magnitude lower than that of magnetite Fe(II). Indeed, HRTEM-EDXS analyses of sorbed and coprecipitated magnetite samples revealed the formation of an amorphous As(III)-rich surface precipitate which dominates As(III) speciation at surface coverages exceeding the maximum site density of vacant tetrahedral sites on the magnetite {111} surface (5.3 µmol/m^2). The origin of this surface precipitate is still poorly understood in the case of sorption experiments. It may be due to the partial dissolution of surface Fe(II) that could precipitate with As(III). Indeed, comparison between sorption and coprecipitation experiments suggests that the nature of the surface precipitate might indeed be similar to the sorption complex since the dissolved As(III) concentrations converge toward similar values in both cases at high As surface coverage (Figure 4). Although such a surface precipitate helps explain the exceptional As(III) sorption capacity of nanomagnetite, it causes a dramatic increase of dissolved As concentration at high surface coverages (up to ~10 µmol/m^2).

Another remarkable property of magnetite toward arsenite sorption found by Ona-Nguema et al. [86] is its ability to rapidly oxidize As(III) to the less toxic As(V) form upon sorption onto nanomagnetite under oxic conditions at neutral pH. Comparison of As(III) sorption in the presence or absence of Fe(II) and under oxic or anoxic conditions indicates that As(III) is likely oxidized by Reactive Oxygen Species (ROS) forming upon oxidation of Fe(II) by dissolved oxygen. Such oxidation reactions involving ROS help to explain the rapid As(III) oxidation in aerated water in presence of zero-valent iron or dissolved Fe(II) ([87] and references theirein). The study by Ona-Nguema et al. [86] showed that As(III) oxidation also occurs in the presence of green-rust. Oxidation reactions involving ROS should thus be considered as potentially important at redox boundaries in the environment and may significantly influence the redox cycling of pollutants.

d. As sorption on green rust: trimer surface species

Green rusts (GRs), $[Fe^{II}_{(1-x)}Fe^{III}_{x}\ (OH)_2]^{x+}\ (CO_3,\ Cl,\ SO_4)^{x-}$ are particularly relevant to reducing environments because they occur in hydromorphic soils and in anoxic iron-rich sediments, and as intermediate Fe(II)-Fe(III)-containing mineral species in the corrosion pathway of zero-valent iron. This mineral may further influence arsenic mobility in groundwaters since it is a common product of the microbial reduction of ferric oxyhydroxides (e.g., Ona-Nguema et al., [86] and references therein). After the pioneering work of Randall et al. [88] which showed the adsorption of As(V) on the edges of GR particles using XAS, only a few studies have addressed the mechanisms of arsenic sorption on - or coprecipitation with - GRs and related layered iron hydroxides. Thoral et al. [89] have shown that nanosized $Fe(OH)_2$ are able to bind As(III) via surface complexes forming on the edges of the octahedral layer, after co-precipitation of As(III) with Fe(II) at high As loading. Jönsson et al. [45] proposed a similar surface sorption mechanism for As(III) on GR, corresponding to edge and double corner As(III) surface complexes.

More recently, we proposed a new mode of As(III) sorption on such layered iron-hydroxides has been which relies on the formation of oligomeric As(III) surface species bound to Fe octahedra via corner sharing linkage [48] These species were first proposed in the case of As(III) co-precipitation with GR and nanosized $Fe(OH)_2$ phases obtained via the bioreduction of As(V)-sorbed lepidocrocite by *Shewanella putrefaciens* [48] (Figure 5). Smaller polymeric species as pairs have been also proposed by Wang et al. [56] for As(III) sorption on GR. According to the theoretical studies of concentrated As solutions by Tossel et al. [90], the most stable configuration for such oligomers would be a $(H_3AsO_3)_3$ trimer ring. On the basis of the small amount of EXAFS data, no definitive clue can be given yet to distinguish between polymeric As(III) surface species and classical edge- and double corner-sharing surface complexes. However, the formation of sorbed oligomeric As(III) species on iron oxides is supported by the almost systematic occurrence of such polymers in the crystal structures of iron arsenite minerals (Figure 5), and could thus be regarded as an alternative mode of As(III) sorption in modeling studies.

Eventually, although GR and related mineral phases are able to adsorb As(III) at their surfaces, the intrinsic affinity of As(III) for theses phases is lower than that observed for magnetite [45], especially at slightly acidic pH. Consequently, although these phases should be able to retard As(III) mobilization in anoxic groundwater, they are expected to be much less efficient than magnetite, However, magnetite would have difficultly forming in natural systems due to the presence of numerous crystal growth inhibitors such as organic acids, silica, and phosphate. In addition, prolonged reducing conditions in well drained soils have

been shown to lead to Fe(II) leaching and subsequent mobilization of arsenic after complete dissolution of iron minerals [25,91].

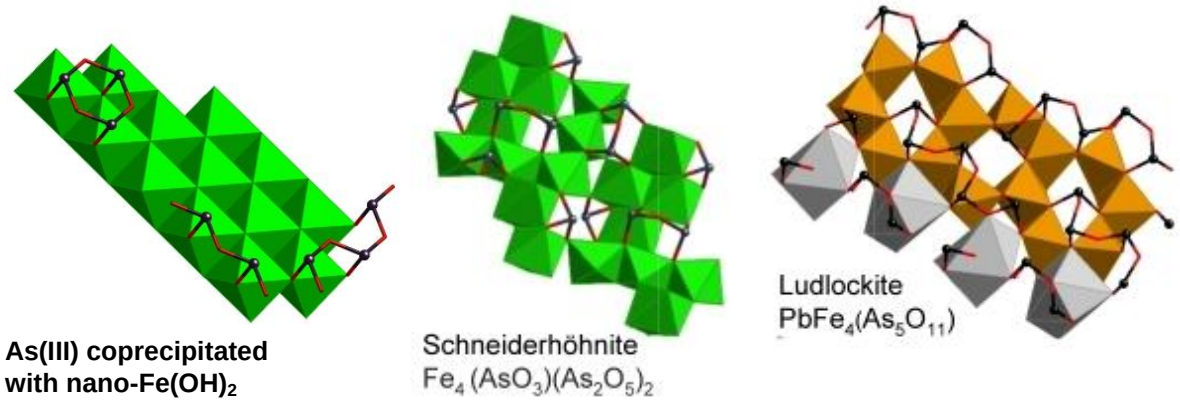

Figure 5. Possible model for oligomeric As(III) species coprecipitated with nanocrystalline $Fe(OH)_2$ particles (after [48]) compared to As(III) dimers and small chains in the structures of Schneiderhönite [92] and ludlockite [93], respectively. Iron(II) and (III) coordination octahedra are displayed in green and orange color, respectively. Arsenic(III) ions are displayed as black spheres. Lead(II) coordination polyhedron is displayed in gray color.

d. As sorption on mackinawite

In ambient anoxic sufidic environments such as aquifers, sediments, or closed marine basins (e.g., the Black Sea) and in presence of ferrous iron, mackinawite, FeS, is the first iron sulfide to precipitate and it constitutes a major component of the empirically defined "acid volatile sulfides" characteristic of such media [94]. Structural characterization of FeS nanoparticulate minerals by analysis of Bragg XRD peaks is limited since diffraction patterns are dominated by broad diffuse scattering [95]. This diffuse component results from extremely small domain sizes as well as from surface relaxation, strain, and complex disorder [96]. In the frame of studies relating to the structural characterization of mackinawite and its reactivity towards As, we used a local structure characterization technique, the Pair Distribution Function (PDF) to analyze both the structure and the particle size of the nanoparticles [97]. The domain size parameter of mackinawite was fit, resulting in 5.2 nm large domains. The specific surface area calculated from these particle sizes is 270 m^2/g [97]. PDF analysis of a freshly precipitated mackinawite showed an average particle size of 2 nm,

which increased with aging to 4–5 nm [98]. Using high-resolution transmission electron microscopy, laminar rectilinear prisms of 2 to 5.7 nm in thickness and 3 to 10.8 nm in length were observed for a similar sample [99]

The surface chemistry of mackinawite and its reactivity to As were also investigated. Acid-base titrations show that the point of zero charge (PZC) of disordered mackinawite lies at pH ~7.5 [95], and mackinawite is not stable below pH 6, the reason why it is one of the main components of the "Acid Volatile Sulfides" [94]. The hydrated disordered mackinawite surface can be best described by strongly acidic monocoordinated and weakly acidic tricoordinated sulfurs. The mono-coordinated sulfur site >Fe-SH determines the acid-base properties at pH ~ PZC. At higher pH, the tricoordinated sulfur determines surface charge changes. Total site density is 4 sites nm^{-2}. The surface chemistry of FeS and its acid-base titration data were adequately described using a surface complexation model by Wolthers et al [95]. Arsenate, AsO_4^{3-}, sorption onto mackinawite is fast. As(V) sorption decreases above the point of zero surface charge of FeS and follows the pH-dependent concentration of positively charged surface species [44]. No redox reaction was observed between the As(V) ions and the mineral surface over the time span of the experiments. These observations suggest that As(V) predominantly forms an outer-sphere complex at the surface of mackinawite. Arsenite, As(III), sorption is not strongly pH-dependent and can be expressed by a Freundlich isotherm. Sorption is fast, although slower than that of As(V). As(III) also forms an outer-sphere complex at the surface of mackinawite. In agreement with previous spectroscopic studies, complexation at low As(V) and As(III) concentrations occurs preferentially at the mono-coordinated sulfide edge sites. Stronger sorption of As(V) than As(III), and thus a higher As(III) mobility, may be reflected in natural anoxic sulfidic waters when disordered mackinawite controls arsenic mobility in ambient sulfidic environments.

f. As sorption and coprecipitation with carbonates (calcite and siderite)

Calcite is an ubiquitous mineral andmost river waters are at equilibrium with calcite [100]. Furthermore, many As-contaminated groundwaters are at equilibrium with siderite ($FeCO_3$) and calcite ($CaCO_3$) [32,57]. The sorptive capacity of siderite towards As is low (Table 1,[45]). Although the specific surface area of these two minerals is low compared to the above discussed minerals, the abundance of carbonate minerals, justifies a close look at their surface chemistry [101] and specifically at their reactions with arsenic.

Sorption of As(III) by calcite was investigated as a function of metalloid concentration, time, and pH [58]. The adsorption mechanism was investigated at a

macroscopic level and the coprecipitation at a nanoscopic level to determine which As species can be incorporated in bulk calcite by substitution at CO_3^{2-} sites [58]. The arsenic sorption isotherm, i.e. the log $\Gamma_{As(III)}$ vs. log ([$As(OH)_3°$]/As_{sat}) plot is S-shaped and has been modeled using an extended version of the surface precipitation model [101,102]. At low concentrations, $As(OH)_3°$ is adsorbed by complexation to surface Ca surface sites, as previously shown by the X-ray standing wave technique [103]. The inflexion point of the isotherm, where $As(OH)_3°$ is limited by the amount of surface sites, yields 6 sites nm^{-2}, in good agreement with crystallographic data. Beyond this value, the amount of sorbed arsenic increases linearly with solution concentration, up to the saturation of arsenic with respect to the precipitation of $CaHAsO_3(s)$, and is interpreted in terms of formation of an ideal solid solution.

The solid solutions formed by calcite and As(III) were examined by high-resolution, synchrotron-based X-ray diffraction, and neutron diffraction, and more recentlu by ESR spectroscopy. The experimental results were compared with results from molecular modeling. The use of the Density Function Theory (DFT) theoretical model allows modeling the effect of the $HAsO_3^{2-}$ substitution at CO_3^{2-} sites on the expansion of the unit cell volume (Figure 6b). This effect of As substitution on calcite unit cell parameters was shown to follow Vegard's law. This allows inferring a value for the amount of As incorporated in the bulk of the mineral; the average value obtained was of [As] = 30 ± 6 mmol/kg. These results extended those published by Cheng et al. [104] on the incorporation of AsO_3^{3-} on the calcite surface to the bulk. Arsenate, where As has a tetrahedral coordination, have also been shown to substitute for CO_3^{2-} groups in calcite [105].

g. As coprecipitation in gypsum

Gypsum is a common sulfate mineral which precipitates in oxic acidic environments. The ability of gypsum ($CaSO_4 \cdot 2H_2O$) to host arsenic atoms in its crystalline structure has been demonstrated through experimental structural studies on the solid solutions formed upon synthetic co-precipitation with arsenic [59]. Neutron and X-ray diffraction methods showed an enlargement of the gypsum unit cell proportional to the concentration of arsenic in the solids and to the pH solution value. The substitution of sulfate ions (SO_4^{2-}) by arsenate ions is shown to be more likely under alkaline conditions, where $HAsO_4^{2-}$ species predominates. A theoretical DFT model of the arsenic-doped gypsum structure reproduces the experimental volume expansion. EXAFS measurements of the local structure around the arsenic atom in the co-precipitated solids confirm solid state substitution and allow some refinement of the local

structure, corroborating the theoretical structure found in the simulations. These results suggest a predominant substitution of CO32- ions by $HAsO_4^{2-}$ species (Figure 6a). The possibility that other species such as AsO_4^{3-} could be incorporated in the bulk of the gypsum structure was also evaluated. The presence of layers of water in the gypsum structure opens the possibility that some hydronium could be present as well, thus compensating the extra charge brought by the unprotonated arsenate species. EXAFS results combined with molecular modeling of the As local structure disregarded this possibility. The charge redistribution within the structure upon substitutions of either the protonated or the unprotonated arsenate species studied by means of Mulliken Population Analyses, demonstrating an increase in the covalency of the interaction between Ca^{2+} and AsO_4^{3-}, whereas the interaction between Ca^{2+} and $HAsO_4^{2-}$ remains predominantly ionic.

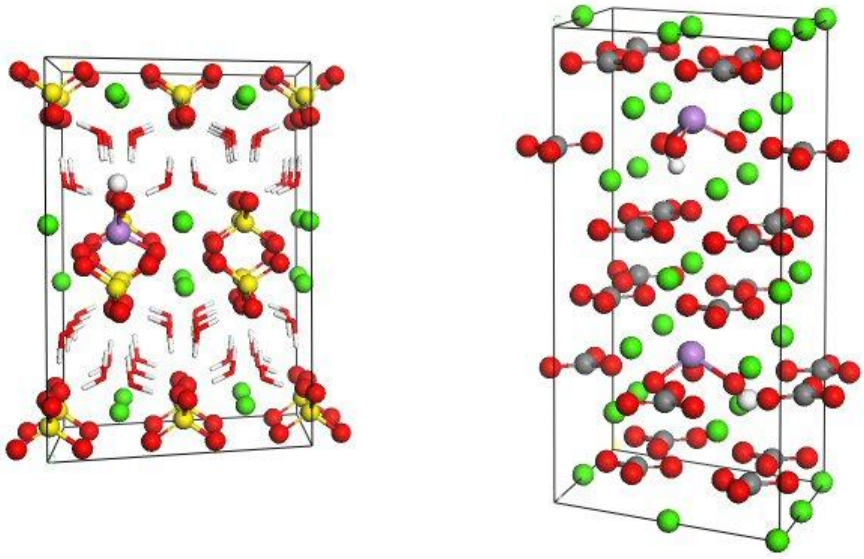

Figure 6. Supercells of gypsum (6a, left) and calcite (6b, right) showing substitutions of sulfate by arsenate (As(V); gypsum) and of carbonate by arsenite oxyanions (As(III); calcite). The green spheres correspond to calcium atoms; red are oxygen; grey are carbon; yellow are sulfur and the red and white sticks in the gypsum structure are structural water molecules.

3. Artifacts in sampling, preparation and spectroscopic analysis

a. Potential oxidation of As(III) and Fe(II) from sampling to analysis.

The quality of both field and lab work related to Fe(II)-rich minerals and their redox reaction with arsenic species heavily depends on the strict control of oxidation artefacts which may occur at any step of the work. Lab work may only be performed in a glove box filled

with nitrogen. Although some people use a mixed H_2/N_2 atmosphere, the "inert" role of H_2 remains an open question, as hydrogen may act as a reductant, e.g. for selenium(IV) ions sorbed on clay mineral particle [57]. The oxygen partial pressure (pO_2) must be monitored continuously by an O_2 sensor and never allowed to exceed 1 ppm. This certified oxygen partial pressure is still high compared to anoxic aquifer conditions and every precaution must be taken to minimize the presence of oxygen which may be introduced e.g. by the standard solutions. The latter should be made inside the glovebox using dry salts and water previously boiled and degassed outside the glovebox. Use of additional O2 traps (such as Fe(OH)2 suspensions or reduced Cr solutions, open to the glovebox atmosphere, are advised to further reduce the O2 content in the glovebox atmosphere. When these strict anoxic conditions are not met, artifacts are observed. For instance As(III) is found to rapidly oxidize in the presence of green-rust and magnetite, upon drying in air, i.e. outside the glovebox, which could be explained by the formation of reactive oxygen species upon reaction of surface Fe(II) with dissolved oxygen [86].

Extreme care must also be taken to prevent sample oxidation during the transport from the glove box to the spectroscopy facilities. Small aliquots (a few mL) of suspensions are typically filtered (Millipore filter 0.022 lm) and the wet pastes then transferred to Mössbauer or XAFS sample holders. The sample holders are sealed with Kapton tape (XAFS spectroscopy) or with epoxy resin (Mössbauer spectroscopy) and placed in small plastic boxes. All these steps are performed in the glove box. The samples are then immediately shock-frozen with liquid N_2 and must be transported to the spectroscopy facilities in a Dewar flask filled with liquid N_2. At the synchrotron facility, they are transferred within 2 minutes from the Dewar to, for example, a closed-cycle He cryostat with He atmosphere and 15 K temperature, used for XAFS measurements. At the Mössbauer facility, the samples are transferred within 1 minute from the Dewar to the Mössbauer bath cryostat with a He gas atmosphere.

Working in the field with anoxic conditions at the middle of a delta with 40°C temperature is even more a challenge. Core samples are particularly delicate to retrieve and to handle. Lake sediments are best obtained like in Sweden in winter time.with the so-called sword technique The hollow sword is introduced gravimetrically in the sediment. It is then filled with liquid CO_2. The sediment freezes around the sword and is brought back frozen to the surface. Since sampling occurs usually in winter from a hole drilled in surface ice the frozen sediment can be directly transferred to the cold room. The same concept is soon to be used to retrieve samples from delta sediments. A specially designed coring tube once it

reaches the desired depth may be sealed on both ends, before retrieval, by freezing with liquid CO_2 or N_2. It is brought back, with its two frozen ends, to the surface where it is immediately introduced in a field campaign glovebox. Pore water, bacteria and particles can then be obtained at each depth without artifact.

The collection of water and particles without oxygen or bacterial contaminations can be done in a cheaper way, using the needle sampler technique [107]. Unconsolidated deposits are drilled in India or Bangladesh using the manual "handflapper" method with 3-m sections of PVC or galvanized iron (GI) pipe [107]. A group of 5 local drillers can drill that way down to 30 m in a given day.At depth intervals of 2-4 m, the drilling is interrupted. The drilling pipes are removed and an empty cylinder is screwed on the bottom pipe. Vacuum is made in this cylinder and an hollow needle is squeezed into the rubber cork which closes the sampling cylinder. The pipes are reintroduced into the borehole, until they touch the bottom of the drill hole. The needle then penetrates a depth ~0.3 m below the bottom of the drill hole. It is then mechanically pushed inside the cylinder. The slurry sample (~ 100 mL) made of groundwater, bacteria and fine particles is then sucked into the cylinder. Once brought back at the surface, and immediately after collection, the headspace of the needle-sampler is purged with N_2. About 5-10 mL of groundwater contained in the needle-sampler is then filtered under a gentle N_2 pressure through a 0.45 μm syringe filter and into acid-leached polyethylene scintillation vials (PolySeal cap) for further element total concentration analysis. In order to preserve arsenic speciation in water, additions of phosphoric acid are further often recommended and this conservation method is discussed in [108]. Another aliquot of groundwater is filtered into scintillation vials that have been rinsed with MQ water only for anionic species measurement. Sediment contained in the N_2 purged needle-sampler is stored in the dark until further processing on the evening of collection.

b. Beam-induced speciation changes: As oxidation on Fe minerals and reduction with organic matter

One of the important limitations of X-ray absorption spectroscopy for studying redox-sensitive elements such as arsenic in dilute samples comes from beam damage. Indeed, although 3d generation synchrotron X-ray sources allows one to reach very low detection limits in concentration (XANES ≈ 0.1 ppm and EXAFS ~ 10 ppm) on very powerful undulator (e.g., ID26 at ESRF) and wiggler beamlines (e.g., BL 11-2 at SSRL), and about ten times higher on focused BM beamlines (e.g., FAME at ESRF), the high photon flux on the

sample may easily change the redox state of the analyzed element during the course of a measurement. In the case of biological or organic samples, the beam can also alter the integrity and molecular structure of the sample. This issue is even more crucial in the case of a focused beam on the micron or nanoscale. Beam damage artifacts are especially important in the case of arsenic. Photo-oxidation and photo-reduction can both be observed and depend on the presence of electron acceptors and donors in the sample matrix, both reactions being activated by the beam. This activation could be explained by the intense ionization of the sample under the X-ray beam, which leads to the photo-emission and migration of electrons that can facilitate electron recombination between electron donors and acceptors. In general, thermodynamically favorable but kinetically limited oxidation and reduction reactions are activated under the beam, as for instance As(III) oxidation by Fe(III) and As(V) reduction by organic molecules. In a given matrix, the proportion of oxidized or reduced As directly depends on the total As concentration and reaches a plateau that might be related to a limiting distance between the electron donor and acceptor atoms. Fortunately, the rates of such beam-activated electron recombinations can be dramatically lowered by decreasing the temperature during beam exposure. For instance, the oxidation of As(III) sorbed Fe(III)-oxides is very fast under the beam at ambient temperature but can be significantly slowed at cryogenic temperatures (preferably below 20K) (Figure 7). XAFS data that requires the averaging of several scans can then be recorded by moving the position of the beam spot between each scan ([50] and references therein). In addition the quick scan mode (< 1 mn) is required at very low As concentrations (< 100 ppm) since significant oxidation of As can occur in a few tens of seconds.

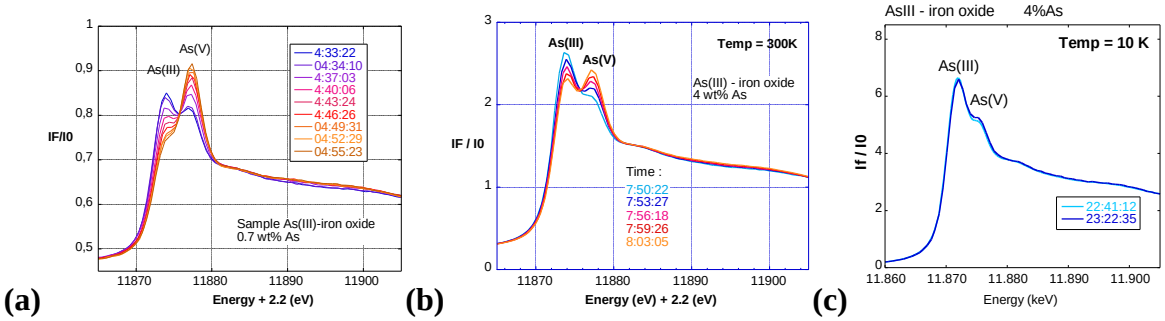

Figure 7. XANES spectra at the As K-edge, for As sorbed onto ferrihydrite recorded in 2002 on ID26 and FAME-BM30B ESRF beamlines. At room temperature, successive XANES scans in quickscan mode (20 seconds per scan) shows that As(III) oxidizes rapidly under the

beam. Such rapid photo-induced oxidation hinders the recording of EXAFS data within a large energy range. The oxidation rate decreases when increasing the As/Fe ratio in the sample, from (a) to (b) and when the recording temperature decreases, i.e. (b) to (c). At very low temperature (c), the oxidation rate is low enough to record a 40 mn long EXAFS scans without significantly modifying the As oxidation state (< 10% oxidation).

4. Water Treatment

a. Drinking water requirements

Because of a constant increase of public awareness concerning the importance of water quality, water regulations have continued to lower the maximum contaminant level (MCL) for pollutants. For instance, in the particular case of arsenic, the World Health Organization (WHO) decided in 2002 to reduce the arsenic standard for drinking water from 50 µg/L to 10 µg/L. Reinforcement of regulations generates a strong need to improve processes to remove pollutants from water and to control water-treatment by-products. A wide range of physical-chemical and biological methods are already used to extract organic and/or inorganic contaminants from polluted waters. Among the most common methods such as coagulation-flocculation, membrane processes and adsorption, the use of inorganic salts as coagulation-flocculation agents such as $AlCl_3$-Al_{13} [109,110,111] and $FeCl_3$-Fe_{24} [112,113,114]polycation species is the most efficient and less expensive process for the removal of colloids and organics in water treatment. But such an approach has the disadvantage of generating a high volume of sewage sludge and results in difficulties to reuse the metals they content..

For water treatment, use a decontamination process that do not generate residuals is an advantage. In the case of arsenic removal, the use of Magnetically Assisted Chemical Separation (MACS) may be of great help [115]. Indeed MACS involve superparamagnetic particles (iron oxide microspheres of 0.1 to 25 µm of diameter) that can be recovered easily, leading to no residual production since iron oxide can be regenerated after adsorption. However, even if micron-sized adsorbents have an internal porosity that increases their specific surface area (SSA), the diffusion within the particles limits their adsorption efficiency. Then the 10 µg/l As MCL is often difficult to achieve by classical techniques .

b. Nanoparticle–based adsorption treatment

As previously discussed, magnetic iron oxide nanoparticles (magnetite and maghemite) represent a new generation of environmental remediation technologies that could provide cost-effective solutions for water and industrial liquid waste treatments. The fact that nano-magnetic iron oxide may adsorb a larger amount of arsenic per unit surface area than other larger particle size adsorbents may be advantageous in reaching the arsenic MCL. However, even if size-dependent reactivity may be a factor, the use of magnetic nanoparticles to remove arsenic exhibits two major advantages: (i) a large specific surface area (SSA) and (ii) the separation of metal-loaded magnetic nano-adsorbents can be achieved via an external magnetic field. For instance, the SSA of an oxide nanoparticle of 10 nm in diameter is ≈100 times larger than the SSA of an oxide particle of 1 μm. It is well known that the surface hydroxyl groups are the chemically reactive entities at the surface of the solid in an aqueous environment. A higher SSA increases the number of available functional groups on the nanoparticle surface. Consequently, for a given mass, the maximum adsorption capacity of ions in solution is higher for nanoparticles than for micron-sized particles.

Most of the published work concerning arsenic removal has focussed on the use of nano-metal oxides or oxyhydroxides (mostly iron and aluminium). Nano-akaganeite [116], ferrihydrite (e.g., [43,60,65,76,117,118]), and other iron nano oxy-hydroxides (e.g., goethite, lepidocrocite [117,119,120,121]), nano zero valent iron [122], and even nano-TiO_2 [123]and many others have been tested as adsorbents for arsenic removal. Nevertheless, the most promising nano-particles need to combine strong adsorption efficiency and magnetic properties for easy removal and regeneration. Accordingly, magnetite and maghemite remain on top of the list.

c. Limitations in recycling nanoparticles

Even if a strong affinity is required between the adsorbent and arsenic to reach the arsenic MCL in water, this may be a drawback in reuse of adsorbents. Indeed, as indicated in above, water treatment process improvements require attainment of a high level of adsorbent material reuse and recycling. However, a strong linkage between arsenic and the adsorbent, similar to that between As and nano-maghemite or nano-magnetite, may limit the regeneration step. Desorption necessitates breaking the chemical linkage between arsenic and the particle surface. For such reactions, acidic or basic baths are needed, which can efficiently desorb arsenic, but such treatments also may alter the adsorbent. Use of corrosive solutions may dramatically increase maintenance costs.

Moreover, for high arsenic concentration waters the high solubility10 mM H_3AsO_3 at pH 7) of the amorphous surface precipitate (present at the surface of nano-magnetite is responsible for a dramatic increase of dissolved As concentrations at high As(III) surface coverage. This mechanism might lower the process efficiency, limits its use to not too contaminated waters and affect the adsorbent renewal capacity.

5. Conclusion and outlook

The sorption mechanisms on a variety of minerals of importance for delta aquifer environment have been reviewed. New mechanisms have been identified which include the formation of an amorphous As(III)-rich surface precipitate on the surface of magnetite, the formation of strong tridentate inner-sphere complexes in vacant tetrahedral sites of magnetite and maghemite nanoparticles and the outer-sphere complexes formed on the surface of hematite. The relevance of each of these mechanisms in natural oxic and anoxic waters and in water treatment or decontamination systems is still to be understood. However, these fundamental investigations have shed light onto fundamental aspects of the mineral/water interfaces, bringing new ideas and thinking about the growth properties of iron oxide nanoparticles to minimize surface tension, the properties of the electric double layer on mineral/water interfaces and the co-existence of inner and outer-sphere complexes, or the existence of polymeric species of As(III), that had been classically underestimated.

Our review suggests that, although the mechanisms by which toxic arsenic aqueous species are trapped in natural and engineered environments on mineral particles are now rather well understood, the integration of these mechanisms in an aquifer broad scale geochemical perspective still need additional work. Of particular interest are studies that include redox properties of As(III)/(V) and Fe(II)/(III). The fact that “amorphous” Fe(II)−Fe(III)-bearing phases are the predominant As scavengers makes understanding redox coupling between these two elements an essential know-how for the development of effective remediation strategies. In this sense, the ongoing efforts to understand the geochemical behavior of As in Southeast Asian groundwaters are good examples of combined fundamental and applied investigations. Studies made during the last 5 years have allowed understanding the coupling of Fe(III) oxyhydroxides reductive dissolution with the mobilization of As(III) toxic species in groundwaters. More research in this field is needed to understand the relative influence of each of the present Fe(II)-bearing solid phases on the redox properties and on the availability of arsenic in these environments.

References

[1] Charlet, L. and Polya, D. (2006) Arsenic in Shallow, Reducing Groundwaters in Southern Asia: An Environmental Health Disaster. *Elements* 2:91-96

[2] Rosen, B. P. Biochemistry of arsenic detoxification. FEBS Lett. 2002, 529 (1), 86–92.

[3] Tamas, M.J., Wysocki, R. (2001) Mechanisms involved in metalloid transport and tolerance acquisition, Current Genetics, 40:2-12

[4] Smith A.H., Marshall G., Yuan Y., Ferreccio C., Liaw J., von Ehrenstein, O., Craig Steinmaus C., Bates M. N., Selvin S. 2006. Increased mortality from lung cancer and bronchiectasis in young adults after exposure to arsenic *in utero* and in early childhood Environ Health Perspect 114: 1293–1296.

[5] Meharg A.A. and Md. Mazibur Rahman Arsenic Contamination of Bangladesh Paddy Field Soils: Implications for Rice Contribution to Arsenic Consumption Environ. Sci. Technol., 2003, 37 (2), pp 229–234.

[6] Ravenscroft P., Brammer H., Richards K. 2009. Arsenic pollution: a global synthesis. Royal Geographical Society with IBG Book Series. Wiley – Blackwell.

[7] Bramer H and Ravenscroft, P. (2009) Arsenic in groundwater: A threat to sustainable agriculture in South and South-east Asia Environment International 36: 647–654

[8] Polya, D. and L. Charlet (2009) Increasing Arsenic Risk? Nature Geoscience 2:383-394.

[9] Winkel, L., Berg, M., Amini, M., Hug, S.S. Johnson C.A. 2008, Predicting groundwater arsenic contamination in Southeast Asia from surface parameters, Nature Geosciences 1: 536-542

[10] Argos M, Kalra T, Rathouz PJ, et al. (2010) Arsenic exposure from drinking water, and all-cause and chronic-disease mortalities in Bangladesh (HEALS): a prospective cohort study. Lancet 6736(10) 60481-3

[11] Gailer, J.,George, G.N., Pickering, I.J., Prince, R.C., Younis, H.S., Winzerling, J. J.(2002) Biliary Excretion of [(GS)2AsSe]- after Intravenous Injection of Rabbits with Arsenite and Selenate Chem. Res. Toxicol., 15 (11) : 1466-1471

[12] Manley SA, George GN, Pickering IJ, Glass RS, Prenner EJ, Yamdagni R, Wu Q, Gailer J; (2006) The seleno bis(S-glutathionyl) arsinium ion is assembled in erythrocyte lysate. *Chemical Research In Toxicology* 19, 601-607.

[13] Chungang Y., Lu S.X., Jie Q., Rosen B.P., Le X.C. (2008) Volatile Arsenic Species Released from *Escherichia coli* Expressing the AsIII S-adenosylmethionine Methyltransferase Gene. *Environmental Science & Technology* 42, 3201-3206.

[14] O'Day P.A. (2006) Chemistry and mineralogy of arsenic. Elements 2, 77-83.

[15] Miot, J.; Morin, G.; Skouri-Panet, F.; Férard, C.; Aubry, E.; Briand, J.; Wang, Y.; Ona-Nguema, G.; Guyot, F.; Brown, Jr., G. E. (2008) XAS Study of Arsenic Coordination in *Euglena gracilis* Exposed to Arsenite. *Environmental Science & Technology* 42(14); 5342-5347.

[16] Miot, J.; Morin, G.; Skouri-Panet, F.; Férard, C.; Poitevin A.; Aubry, E.; Ona-Nguema G..; Juillot F. ; Guyot, F.; Brown, Jr., G. E. (2009) Speciation of Arsenic in *Euglena gracilis* Cells Exposed to As(V). *Environmental Science and Technology* 43, 3315-3321

[17] Métral, J., Charlet, L., Bureau, S., Basu Mallik, S., Chakraborty, S., M Ahmed K., Rahman, MW, Cheng, Z. van Geen, A. (2008) Comparison of dissolved and particulate arsenic distributions in shallow aquifers of Chakdaha, India, and Araihazar, Bangladesh *Geochemical Transactions* 2008, 9:1-18.

[18] Polizzoto, M.L., Kocar, B.D., Benner, S.G., Sampson, M., Fendorf, S. (2008) Near-surface wetland sediments as a source of arsenic release to ground water in Asia Nature 454: 505-509

[19] Lawson, M. (2010) Isotopic Tracers of Surface Derived Components in Arsenic Rich Shallow Aquifers of South and South East Asia. Ph.D. thesis, University of Manchester

[20] Burnol, A., Garrido, F., Baranger, P., Joulian, C., Dictor, M., Bodenan, F., Morin, G. and Charlet, L. (2007) Decoupling of arsenic and iron release from ferrihydrite suspension under reducing conditions: a biogeochemical model. *Geochemical Transactions* **8,** 12.

[21] Van Geen, A., Rose, J., Thoral, S., Garnier, J. M., Zheng, Y., and Bottero, J. Y. (2004) Decoupling of As and Fe release to Bangladesh groundwater under reducing conditions. Part II: Evidence from sediment incubations, *Geochimica et Cosmochimica Acta, 68*, 3475-3486.

[22] Fendorf, S.,Michael, H.A., van Geen, A. (2010) Does the distribution of arsenic in groundwater change over time in South and Southeast Asia? Biogeochemical and hydrological factors to consider. Science

[23] Morin G. and Calas G. (2006) Arsenic in soils, mine tailings, and former industrial sites. *Elements* 2 (2), 97-101.

[24] Charlet, L., Chakraborty, S., Appelo, C.A.J., Roman-Ross, G., Nath, B., Ansari, A.A., Musso, M. Chatterjee, D., and Basu Mallik, S. (2007) Chemodynamics of an Arsenic "hotspot" in a West Bengal aquifer: A field and reactive transport modeling study. *Applied Geochem*. 22 (2007) 1273–1292.

[25] Tufano, K.J.; Fendorf, S. Confounding impacts of iron reduction on arsenic retention. *Environ. Sci. Technol.* **2008**, *42*, 4777-4783.

[26] Root, R. A.; Dixit, S.; Campbell, K. M.; Jew, A. D.; Hering, J. G.; O'Day, P. A., (2007) Arsenic sequestration by sorption processes in high-iron sediments. *Geochim. Cosmochim. Acta 71*, (23), 5782-5803.

[27] Ona-Nguema, G**.**, G. Morin, Y. Wang, N. Menguy, F. Juillot, L. Olivi, G. Aquilanti, M. Abdelmoula, C. Ruby, F. Guyot, G. Calas, and G.E. Brown, Jr. (2009) Arsenic sequestration at the surface of nano-$Fe(OH)_2$, ferrous-carbonate hydroxide, and green-rust after bioreduction of arsenic-sorbed lepidocrocite by *Shewanella putrefaciens*. *Geochim. Cosmochim. Acta* **73**(5), 1359-1381.

[28] Bostick, B. C. and Fendorf S. Arsenite sorption on troilite (FeS) and pyrite (FeS_2). *Geochim. Cosmochim. Acta* **2003**, *67*, 909 –921.

[29] Burnol, A. and Charlet, L. (2010) Fe(II)−Fe(III)-Bearing Phases As a Mineralogical Control on the Heterogeneity of Arsenic in Southeast Asian Groundwater. *Environmental Science & Technology* doi: 10.1021/es100280h

[30] Islam, F. S.; Gault, A. G.; Boothman, C.; Polya, D. A.; Charnock, J. M.; Chat terjee, D.; Lloyd, J. R. Role of metal-reducing bacteria in arsenic release from Bengal delta sediments. Nature 2004, 430, 68–71.

[31] Michel F. M., Ehm L., Liu G., Han W. Q., Antao S. M., Chupas P. J., Lee P. L., Knorr K., Eulert H., Kim J., Grey C. P., Celestian A. J., Gillow O. J., Schoonen M. A. A., Strongin D. R., and Parise J. B. (2007) Similarities in 2- and 6-Line Ferrihydrite Based on Pair Distribution Function Analysis of X-ray Total Scattering. Chem. Matter. 19, 1489-1496.

[32] Nath, B.; Chakraborty, S.; Burnol, A.; Stu¨ben, D.; Chatterjee, D.; Charlet, L. (2009) Mobility of arsenic in the sub-surface environment: An integrated hydrogeochemical study and sorption model of the sandy aquifer materials. *J. Hydrol.* 364, 236–248.

[33] Kocar, B. D.; Fendorf, S. Thermodynamic constraints on reductive reactions influencing the biogeochemistry of arsenic in soils and sediments. *Environ. Sci. Technol.* 2009, 43, 4871– 4877.

[34] Pallud, C., Kausch, M., Fendorf, S. and C. Meile. 2010. Patterns and spatial modeling of reductive ferrihydrite transformation observed in artificial soil aggregates. Environ. Sci. Technol. 44: 74-79.

[35] Pallud, C., Masue-Slowey, Y. and S. Fendorf. 2010. Aggregate-scale spatial heterogeneity in reductive transformation of ferrihydrite resulting from coupled biogeochemical and physical processes. Geochim. Cosmochim. Acta. 74: 2811-2825.

[36] Masue-Slowey, Y. Kocar, B.D., Bea Jofré, S.A., K. Mayer, U. Fendorf S. Transport Implications Resulting from Internal Redistribution of Arsenic and Iron within Constructed Soil Aggregates Environment Science and Technology (in press)

[37] Goldberg, S. Competitive adsorption of arsenate and arsenite on oxides and clay minerals. *Soil Sci. Soc. Am. J.*, **2002**, *66*, 413–421

[38] Benzerara K., G. Morin, T.H. Yoon, J. Miot, T. Tyliszczak, C. Casiot, O. Bruneel, F. Farges, G.E. Brown Jr. (2008) Nanoscale study of As biomineralization in an acid mine drainage system. *Geochimica et Cosmochimica Acta* 72, 3949-3963.

[39] Inskeep WP, Macur RE, Harrison G, Bostick BC, Fendorf S (2004) Biomineralization of As(V)-hydrous ferric oxyhydroxide in microbial mats of an acid-sulfate-chloride geothermal spring, Yellowstone National Park. *Geochimica et Cosmochimica Acta* 68: 3141–3155.

[40] Morin G., Rousse G., Elkaim E. (2007) Crystal structure of tooeleite, a new iron arsenite hydroxysulfate relevant of acid mine drainage. *American mineralogist* 92, 193-197.

[41] Egal M., Casiot C., Morin G., Parmentier M., Bruneel O., Lebrun S., Elbaz-Poulichet F. (2009) Kinetic control on the formation of tooeleite, schwertmannite and jarosite by *Acidithiobacillus ferrooxidans* strains in an As(III)-rich acid mine water. *Chemical Geology* 265, 432-441.

[42] Hohmann C., Winkler E., Morin G., Kappler A. (2010) Anaerobic Fe(II)-oxidizing bacteria show As resistance and immobilize As during Fe(III) mineral precipitation. *Environmental Science & Technology* 44, 94-101.

[43] Dixit, S., and Hering, J. G. Comparison of arsenic(V) and arsenic(III) sorption onto iron oxide minerals: Implications for arsenic mobility, *Environmental Science & Technology,* (2003) *37*, 4182-4189.

[44] Wolthers M., Charlet L., Van der Weijden C.H., Van der Linde P.R., Rickard D. (2005b) Arsenic mobility in the ambient sulphidic environment: sorption of Arsenic (V) and Arsenic (III) onto disordered mackinawite *Geochim. Cosmochim Acta* 69 (14): 3483-3492

[45] Jönsson, J.; Sherman, D. M. Sorption of As(III) and As(V) to siderite, green rust (fougerite) and magnetite: Implications for arsenic release in anoxic groundwaters.

Chem. Geol. 2008, 255 (1-2), 173–181.

[46] Thinnappan V., Merrifield C. M., Islam F. S., Polya D. A., Wincott P. and Wogelius R. A. (2008) A combined experimental study of vivianite and As (V) reactivity in the pH range 2–11. Appl. Geochem.23, 3187-3204.

[47] Chakraborty, S., Wolthers, M., Chatterjee, D., Charlet, L. (2007) Adsorption of Arsenite and Arsenate on Muscovite & Biotite Mica Journal of Colloid and Interface Science 309 :392-401.

[48] Ona-Nguema, G., Morin, G., Juillot, F., Calas, G., and Brown, G. E. EXAFS analysis of arsenite adsorption onto two-line ferrihydrite, hematite, goethite, and lepidocrocite, Environmental Science & Technology,(2005) 39, 9147-9155.

[49] Auffan, M., Rose, J., Proux, O., Borschneck, D., Masion, A., Chaurand, P., Hazemann, J. L., Chaneac, C., Jolivet, J. P., Wiesner, M. R., Van Geen, A., and Bottero, J. Y. Enhanced adsorption of arsenic onto maghemites nanoparticles: As(III) as a probe of the surface structure and heterogeneity, *Langmuir*, (2008) *24*, 3215-3222.

[50] Morin G., Ona-Nguema G., Wang Y. Menguy N., Juillot F., Proux O., Guyot F., Calas G., Brown JR. G.E. (2008) EXAFS analysis of arsenite and arsenate adsorption on maghemite. *Environmental Science and Technology* 42, 2361-2366.

[51] Yean, S., Cong, L., Yavuz, C. T., Mayo, J. T., Yu, W. W., Kan, A. T., Colvin, V. L., and Tomson, M. B. (2005) Effect of magnetic particle size on adsorption and desorption of arsenite and arsenate, *Journal of Matererial Research 20*, 3255-3264.

[52] Wang, Y. H., Morin, G., Ona-Nguema, G., Menguy, N., Juillot, F., Aubry, E., Guyot, F., Calas, G., and Brown, G. E. Arsenite sorption at the magnetite-water interface during aqueous precipitation of magnetite: EXAFS evidence for a new arsenite surface complex, *Geochimica et Cosmochimica Acta*, (2008) *72*, 2573-2586.

[53] Morin, G., Wang, Y. H., Ona-Nguema, G., Juillot, F., Calas, G., Menguy, N., Aubry, E., Bargar, J. R., and Brown, G. E. EXAFS and HRTEM Evidence for As(III)-Containing Surface Precipitates on Nanocrystalline Magnetite: Implications for As Sequestration, *Langmuir*, (2009) *25*, 9119-9128.

[54] Auffan M., Shipley H.J., Yean S., Kan A.T., Tomson M., Rose J., Bottero J-Y., (2007) 'Nanomaterials as Adsorbant' in 'Environmental Nanotechnology: Applications and Impacts of Nanomaterials' (Mc Graw Hill, Wiesner and Bottero Ed.)

[55] Auffan, M., Rose, J., Bottero, J. Y., Lowry, G. V., Jolivet, J. P., and Wiesner, M. R. Towards a definition of inorganic nanoparticles from an environmental, health and safety perspective, *Nature Nanotechnology*, (2009) *4*, 634-641.

[56] Wang Y., Morin G., Ona-Nguema G., Juillot J., Guyot F., Calas G., Brown Jr. G.E. (2010) Evidence for Different Surface Speciation of Arsenite and Arsenate on Green Rust: an EXAFS and XANES study. *Environmental Science & Technology* 44, 109-115.

[57] Charlet L., Chakraborty S., Varma S., Tournassat C., Wolthers M., Chatterjee D. Roman Ross G. (2005) Adsorption and heterogeneous reduction of arsenic at the phyllosilicate-water interface. Advances in Arsenic Research: Integration of Experimental and Observational Studies and Implications for Mitigation. ACS Symposium Series Vol. 915, American Chemical Society, Editors: Peggy A. O'Day, Dimitrios Vlassopoulos, Xiaoguang Meng, Liane G. Benning pp.41-59.

[58] Roman-Ross, G., Cuello, G.J., Turrillas, X., Fernandez-Martınez, A., Charlet, L. (2006) Arsenite sorption and co-precipitation with calcite *Chemical Geology* 233: 328-336.

[59] Fernandez-Martinez, A., Cuello, G.J., Johnson, M.R., Bardelli, F., Román-Ross, G.,. Charlet, L., Turillas, X (2008) Arsenate incorporation in gypsum probed by X-Ray scattering, neutron diffraction, Density Function Theory modeling. J. Phys. Chem. A 112, 5159–5166.

[60] Waychunas, G. A., Rea, B. A., Fuller, C. C., and Davis, J. A. Surface-Chemistry Of Ferrihydrite .1. Exafs Studies Of The Geometry Of Coprecipitated And Adsorbed Arsenate, *Geochimica et Cosmochimica Acta*,(1993) *57*, 2251-2269.

[61] Manning, B. A., Fendorf, S. E., and Goldberg, S. (1998) Surface structures and stability of arsenic(III) on goethite: Spectroscopic evidence for inner-sphere complexes, *Environmental Science & Technology 32*, 2383-2388.

[62] Foster AL, Brown Jr GE, Tingle TN, Parks GA (1998) Quantitative arsenic speciation in mine tailings using X-ray absorption spectroscopy. *American Mineralogist* 83, 553–568.

[63] Morin G, Lecocq D, Juillot F, Calas G, Ildefonse P, Belin S, Briois V, Dillmann P, Chevallier P, Gauthier C, Sole A, Petit PE, Borensztajn S (2002) EXAFS evidence of sorbed arsenic(V) and pharmacosiderite in a soil overlying the Echassieres geochemical anomaly, Allier, France. Bulletin de la Société Géologique de France 173: 281-291.

[64] Cancès B., Juillot F., Morin G., Laperche V., Polya D.,Vaughan D.J., Hazemann J.L., Proux O., Brown Jr. G. E. and Calas G. (2008) Change in arsenic speciation through a contaminated soil profile: a XAS based study. *Science of the Total Environm*ent 397, 178-189.

[65] Ona-Nguema G, Morin G, Juillot F, Brown Jr. GE, Calas G (2005) EXAFS analysis of Arsenic(III) sorption onto 2-line ferrihydrite, hematite, gœthite, and lepidocrocite under anoxic conditions. Influence of the surface structure. *Environmental Science and Technology* 39, 9147-9155.

[66] Sherman, DM; Randall, SR (2003) Surface complexation of arsenic(V) to iron(III) (hydr)oxides: Structural mechanism from ab initio molecular geometries and EXAFS spectroscopy. *Geochim. Cosmochim. Acta* 67, 4223-4230.

[67] Cancès B., Juillot F., Morin G., Laperche V., Alvarez L., Proux O., Hazemann J-L, Brown Jr. G.E., Calas G. (2005) XAS evidence of As(V) association with iron oxyhydroxides in a contaminated soil at a former arsenical pesticide processing plant. *Environmental Science and Technology* 39, 9398-9405.

[68] Cancès B., Juillot F., Morin G., Laperche V., Polya D.,Vaughan D.J., Hazemann J.L., Proux O., Brown Jr. G. E. and Calas G. (2008) Change in arsenic speciation through a contaminated soil profile: a XAS based study. *Science of the Total Environm*ent 397, 178-189.

[69] Catalano JG, Park C, Fenter P, Zhang Z (2008) Simultaneous inner- and outer-sphere arsenate adsorption on corundum and hematite. *Geochim. Cosmochim. Acta* 72, 1986-2004.

[70] Bargar, J.R., S.N. Towle, G.E. Brown, Jr., and G.A. Parks (1996) Outer-sphere lead(II) adsorbed at specific surface sites on single crystal α-alumina. Geochim. Cosmochim. Acta **60**, 3541-3547.

[71] Krause E., Ettel V.A. (1989) Solubilities and stabilities of ferric arsenate compounds. *Hydrometallurgy* 22, 311-337.

[72] Robins RG, Glastras MV. (1987) The precipitation of arsenic from aqueous solution in relation to disposal from hydrometallurgical processes. Proceedings, research and development in extractive metallurgy. Aust. Inst. Min. Metall., Adelaide, 223–7.

[73] Tozawa K, Umetsu Y, Nishimura T. (1978) Hydrometallurgical recovery or removal of arsenic from copper smelter by-products. 107th AIME annu. meet., Denver, Colorado, 78–84

[74] Vircikova E, Molnar L, Lech P, Reitznerova E. (1985) Solubilities of amorphous Fe–As precipitates. Hydrometallurgy 38:111–23.

[75] Pierce LM, Moore BM. (1982) Adsorption of arsenite and arsenate on amorphous iron hydroxide. *Water Res* 16, 1247–53.

[76] Raven, K. P., Jain, A., and Loeppert, R. H. (1998) Arsenite and arsenate adsorption on ferrihydrite: Kinetics, equilibrium, and adsorption envelopes, *Environmental Science & Technology 32*, 344-349.

[77] Yean, S., Cong, L., Yavuz, C. T., Mayo, J. T., Yu, W. W., Kan, A. T., Colvin, V. L., and Tomson, M. B. (2005) Effect of magnetic particle size on adsorption and desorption of arsenite and arsenate, *Journal of Matererial Research* 20, 3255-3264.

[78] Ha, J., T.P. Trainor, F. Farges, and G.E. Brown, Jr. (2009) Interaction of Zn(II) with hematite nanoparticles and microparticles: Part 1. EXAFS spectroscopy study of Zn(II) adsorption and precipitation. Langmuir **25**(10), 5574-5585.

[79] Brice-Profeta, S., Arrio, M. A., Tronc, E., Menguy, N., Letard, I., Cartier dit Moulin, C., Nogues, M., Chaneac, C., Jolivet, J. P., and Sainctavit, P. Magnetic order in γ-Fe_2O_3 nanoparticles: an XMCD study, Journal of Magnetism and Magnetic Materials, (2005) 288, 354–365.

[80] Towle, S.N. J.R. Bargar, G.E. Brown, Jr., and G.A. Parks (1997) Surface precipitation of Co(II) (aq) on Al_2O_3. J. Colloid Interface Sci. **187**, 62-82.

[81] Scheidegger, A.M., G.M. Lamble, and D.L. Sparks (1997) Spectroscopic evidence for the formation of mixed-cation hydroxide phases upon metal sorption on clays and aluminum oxides. J. Colloid Interface Sci. **186**, 118-128

[82] Missana, T., Alonso, U., Scheinost, A. C., Granizo, N., and Garcia-Gutierrez, M. Selenite retention by nanocrystalline magnetite: Role of adsorption, reduction and dissolution/co-precipitation processes, *Geochimica et Cosmochimica Acta,* (2009) *73*, 6205- 6217.

[83] Yavuz, C. T.; Mayo, J. T.; Yu, W. W.; Prakash, A.; Falkner, J. C.; Yean, S.; Cong ,L.; Shipley, H. J.; Kan, A.; Tomson, M.; Natelson, D.; Colvin V. L. Low-field magnetic separation of monodisperse Fe_3O_4 nanocrystals. *Science* **2006**, *314*, 964-967.

[84] Neuberger, C. S.; Helz G. R. (2005) Arsenic(III) carbonate complexing *Appl. Geochem. 20*, 1218-1225.

[85] Kirsch R., Scheinost A.C., Rossberg A., Banerjee D., Charlet L. (2008) Reduction of antimony by nano-particulate magnetite and mackinawite. *Mineralogical Magazine* 72(1), 27-31.

[86] Ona-Nguema G. Morin G., Wang Y., Foster. A. Juillot F., Calas G., Brown Jr. G.E. (2010) XANES evidence for rapid Arsenic(III) Oxidation at Magnetite, and Ferrihydrite Surfaces by dissolved O_2, via Fe^{2+}-Mediated Reactions. *Environmental Science and*

Technology 44 (14), 5416–5422.

[87] Hug, S. J.; Leupin, O. (2003) Iron-catalyzed oxidation of arsenic(III) by oxygen and by hydrogen peroxide: pH-dependent formation of oxidants in the Fenton reaction. *Environ. Sci. Technol. 37*, 2734-2742.

[88] Randall, S. R.; Sherman, D. M.; Ragnarsdottir, K. V. Sorption of As(V) on green rust ($Fe^{II}_4Fe^{III}_2(OH)_{12}SO_4 \cdot 3H_2O$) and lepidocrocite (gamma-FeOOH): Surface complexes from EXAFS spectroscopy. Geochim. Cosmochim. Acta 2001, 65, 1015–1023.

[89] Thoral, S.; Rose, J.; Garnier, J. M.; Van Geen, A.; Refait, P.; Traverse, A.; Fonda, E.; Nahon, D.; Bottero, J. Y. XAS study of iron and arsenic speciation during Fe(II) oxidation in the presence of As(III). Environ. Sci. Technol. 2005, 39 (24), 9478–9485.

[90] Tossel J.A. (1997) Theoretical studies on arsenic oxide and hydroxide species in minerals and in aqueous solution. *Geochimica et Cosmochimica Acta* 61, 1613-1623.

[91] Fakih M., Davranche M., Dia A., Nowack B., Morin G., Petitjean P., Châtellier X., Gruau G. (2009) Environmental impact of As(V)-Fe oxyhydroxide reductive dissolution: An experimental insight. *Chemical Geology* 259, 290-303.

[92] Hawthorne, F. C. (1985) Schneiderhöhnite, $Fe^{2+}(Fe^{3+})_3(As^{3+})_5O_{13}$, A densely packed arsenite structure. *Can. Mineral. 23*, 675-679.

[93] Cooper, M. A.; Hawthorne, F. C. (1996) The crystal structure of ludlockite, $Pb(Fe^{3+})_4(As^{3+})_{10}O_{22}$, the mineral with pentameric arsenite groups and orange hair. *Can. Mineral. 34*, 79-89.

[94] Rickards, D., and Morse, J.W. (2005) Acid Volatile Sulfides (AVS) Marine Chemistry 97, 141–197.

[95] Wolthers M., Charlet L., Van der Linde P.R., Rickard D., Van der Weijden C.H. (2005a) The surface chemistry of disordered mackinawite *Geochim. Cosmochim Acta* 69 (14): 3469-3481.

[96] Gilbert B., Huang F., Zhang H. Z., Waychunas G. A. and Banfield J. F. (2004) Nanoparticles: strained and stiff. Science 305, 651-654

[97] Scheinost, A.C., Kirsch, R., Banerjee, D., H., Fernandez-Martinez, A., Zaenker, H., Funke, H., Charlet, L. (2008) X-ray absorption and photoelectron spectroscopy investigation of selenite reduction by FeII–bearing minerals J. Cont. Hydr. 102: 228–245

[98] Michel, F.M., Antao, S.M., Chupas, P.J., Lee, P.L., Parise, J.B., Schoonen, M.A.A., 2005. Short- to medium-range atomic order and crystallite size of the initial FeS precipitate from pair distribution function analysis. Chem. Mater. 17 (25), 6246–6255

[99] Ohfuji, H., Rickard, D., 2006. High resolution transmission electron microscopic study of synthetic nanocrystalline mackinawite. Earth Planet. Sci. Lett. 241 (1–2), 227–233.

[100] Stumm W. and Morgan J. J. (1981) Aquatic chemistry: an introduction emphasizing chemical equilibria in natural waters. New York: Wiley-Interscience, 583 pp.

[101] Wolthers M., Charlet L., Van Cappellen P. (2008) The surface chemistry of divalent metal carbonate minerals; a critical assessment of surface charge and potential data using the charge distribution multi-site ion complexation model. *American. J. Science* 308:905-941

[102] Farley, K.J., Dzombak, D.A., Morel, F.F.M., 1985. A surface precipitation model for the sorption of cations on metal oxides. Journal of Colloid and Interface Science 106 (227–242)

[103] Wersin, P., Charlet, L., Kathein, R., Stumm, W., 1989. From adsorption to precipitation: sorption of Mn^{2+} to $FeCO_3$(s). Geochimica et Cosmochimica Acta 53, 2787–2796.

[104] Cheng, L.W., Fenter, P., Sturchio, N.C., Zhong, Z., Bedzyk, M.J., 1999. X-ray standing wave study of arsenite incorporation at the calcite surface. Geochimica et Cosmochimica Acta 63 (19–20), 3153–3157

[105] Alexandratos, V.G., E.J. Elzinga, and R.J. Reeder (2007) Arsenate uptake by calcite: Macroscopic and spectroscopic characterization of adsorption and incorporation mechanisms. Geochim. Cosmochim. Acta 71, 4172-4187.

[106] Géhin, A., Grenèche, J.-M., C. Tournassat, C., Brendlé, J., Rancourt, D.G. and L. Charlet (2007) Reversible surface-sorption-induced electron-transfer oxidation of Fe(II) at reactive sites on a synthetic clay mineral *Geochimica et Cosmochimica Acta* 71 863–876

[107] Van Geen., Protus, T., Cheng, Z., Horneman, A ., Seddique , A.A., Hoque, M. A ., Ahmed, K. M . (2004) Testing groundwater for arsenic in Bangladesh before installing a well. Environmental Science and Technology 38, 6783-6789

[108] Daus, B., Weiss, H. , Mattusch, J., Wennrich, R. Preservation of arsenic species in water samples using phosphoric acid - Limitations and long-term stability, Talanta, 69/2 (2006) 430-434.

[109] Bottero, J. Y., Cases, J. M., Fiessinger, F., and Poirier, J. E. Studies Of Hydrolyzed Aluminum-Chloride Solutions .1. Nature Of Aluminum Species And Composition Of Aqueous-Solutions, *Journal of physical chemistry*, (1980) *84*, 2933-2939.

[110] Bottero, J. Y., Tchoubar, D., Cases, J. M., and Flessinger, F. Investigation Of The Hydrolysis Of Aqueous-Solutions Of Aluminum-Chloride .2. Nature And Structure By Small-Angle X-Ray-Scattering, *Journal of physical chemistry*, (1982) *86*, 3667-3673.

[111] Masion, A., Vilge-Ritter, A., Rose, J., Stone, W. E. E., Teppen, B. J., Rybacki, D., and Bottero, J. Y. (2000) Coagulation-flocculation of natural organic matter with Al salts: Speciation and structure of the aggregates, *Environmental Science & Technology* 34, 3242-3246.

[112] Bottero, J. Y., Arnaud, M., Villieras, F., Michot, L. J., Dedonato, P., and Francois, M. Surface And Textural Heterogeneity Of Fresh Hydrous Ferric Oxides In Water And In The Dry State, *Journal of Colloid and Interface Science*, (1993) *159*, 45-52.

[113] Bottero, J. Y., Manceau, A., Villieras, F., and Tchoubar, D. Structure and Mechanisms of Formation of FeOOH(Cl) Polymers, *Langmuir*, (1994) *10*, 316-319.

[114] Vilge-Ritter, A., Rose, J., Masion, A., Bottero, J.-Y., and Laine, J.-M. (1999) Chemistry and structure od aggregates formed with Fe-salts and natural organnic matter, Colloids and surfaces A 147, 297-308.

[115] Ngomsik, A.-F., Bee, A., Draye, M., Cote, G., and Cabuil, V. (2005) Magnetic nano- and microparticles for metal removal and environmental applications: A review, *Comptes Rendus Chimie 8*, 963.

[116]Deliyanni, E. A., Bakoyannakis, D. N., Zouboulis, A. I., and Matis, K. A. Sorption of As(V) ions by akaganeite-type nanocrystals, *Chemosphere*, (2003) *50*, 155-163.

[117] Wilkie, J. A., and Hering, J. G. Adsorption of arsenic onto hydrous ferric oxide: Effects of adsorbate/adsorbent ratios and co-occurring solutes, *Colloids and Surfaces a-Physicochemical and Engineering Aspects*,(1996) *107*, 97-110.

[118] Jain, A., Raven, K. P., and Loeppert, R. H. Arsenite and arsenate adsorption on ferrihydrite: Surface charge reduction and net OH- release stoichiometry, Environmental Science & Technology,(1999) 33, 1179-1184.

[119] Farquhar, M. L., Charnock, J. M., Livens, F. R., and Vaughan, D. J. Mechanisms of arsenic uptake from aqueous solution by interaction with goethite, lepidocrocite, mackinawite, and pyrite: An X-ray absorption spectroscopy study, *Environmental Science & Technology*,(2002) *36*, 1757-1762.

[120] Manning, B. A.; Hunt, M. L.; Amrhein, C.; Yarmoff, J. A. (2002) Arsenic(III) and arsenic(V) reactions with zerovalent iron corrosion products. *Environ Sci Technol 36*, 5455-5461.

[121] Sun, X. H., and Doner, H. E. Adsorption and oxidation of arsenite on goethite, *Soil Science*,(1998) *163*, 278-287.

[122] Kanel, S. R., Manning, B., Charlet, L., and Choi, H. Removal of arsenic(III) from groundwater by nanoscale zero-valent iron, Environmental Science & Technology,(2005) 39, 1291-1298.

[123] Jegadeesan, G., Al-Abed, S. R., Sundaram, V., Choi, H., Scheckel, K. G., and Dionysiou, D. D. Arsenic sorption on TiO2 nanoparticles: Size and crystallinity effects, Water Research,(2010) 44, 965-973.

Table 1: Kd of As(III) and As(V) onto Fe(II)-Fe(III)-bearing phases derived from sorption edge experiments (pH 7 and 7.5)

Fe(II)-Fe(III)-bearing phases	Solid g/L	Kd L/g As(III) at pH 7 (pH 7.5)	Kd L/g As(V) at pH 7 (pH 7.5)	Ref
HFO	0.03	85.72 (87.79)	49.3 (37.59)	[43]
Goethite	0.5	14.46 (16.1)	8.05 (5.39)	[43]
mackinawite	0.044	2	9	[44]
siderite	2.5	0.28 (0.36)	3.36 (1.86)	[45]
magnetite	3.1	0.08 (0.20)	(8.89)	[45]
	0.5	1.85 (2.02)	-	[43]
fougerite	4.5	0.12 (0.42)	-	[45]
vivianite	2.5	-	0.18 (0.18)	[46]
Muscovite [a]	4.1	0.36 (0.13)	0.36 (0.13)	[47]
Biotite [a]	4.25	0.97 (0.31)	3.4 (0.9)	[47]

[a] derived from constant capacity (CC) modeling of adsorption edge experiments